HHS Public Access

Author manuscript

Microcirculation. Author manuscript; available in PMC 2019 January 01.

Published in final edited form as:

Microcirculation. 2018 January ; 25(1): . doi:10.1111/micc.12436.

The yin and yang of K_V channels in cerebral small vessel pathologies

Masayo Koide[1], **Arash Moshkforoush**[2], **Nikolaos M. Tsoukias**[2], **David C. Hill-Eubanks**[1], **George C. Wellman**[1], **Mark T. Nelson**[1,3], and **Fabrice Dabertrand**[1]

[1]Department of Pharmacology, University of Vermont, Burlington, Vermont, USA

[2]Department of Biomedical Engineering, Florida International University, Miami, Florida, USA

[3]Institute of Cardiovascular Sciences, University of Manchester, Manchester, UK

Abstract

Cerebral small vessel diseases (SVDs) encompass a group of genetic and sporadic pathological processes leading to brain lesions, cognitive decline, and stroke. There is no specific treatment for SVDs, which progress silently for years before becoming clinically symptomatic. Here, we examine parallels in the functional defects of parenchymal arterioles in CADASIL, a monogenic form of SVD, and in response to subarachnoid hemorrhage, a common type of hemorrhagic stroke that also targets the brain microvasculature. Both animal models exhibit dysregulation of the voltage-gated potassium channel, K_V1, in arteriolar myocytes, an impairment that compromises responses to vasoactive stimuli and impacts cerebral blood flow autoregulation and local dilatory responses to neuronal activity (neurovascular coupling). However, the extent to which this channelopathy-like defect ultimately contributes to these pathologies is unknown. Combining experimental data with computational modeling, we describe the role of K_V1 channels in the regulation of myocyte membrane potential at rest and during the modest increase in extracellular potassium associated with neurovascular coupling. We conclude that parenchymal arteriole resting membrane potential and myogenic tone depend strongly on $K_V1.2/1.5$ channel density, and that reciprocal changes in K_V channel density in CADASIL and subarachnoid hemorrhage produce opposite effects on extracellular potassium-mediated dilation during neurovascular coupling.

Keywords

voltage-gated potassium channel; cerebral blood flow; cerebral small vessel disease; CADASIL; subarachnoid hemorrhage

Address for correspondence: Fabrice Dabertrand, Ph.D., Department of Pharmacology, College of Medicine, University of Vermont, Given Building, Room B-333A, 89 Beaumont Avenue, Burlington, VT 05405-0068, USA. f.dabertrand@gmail.com.
DR. FABRICE DABERTRAND (Orcid ID : 0000-0003-2541-9185)

CONFLICT OF INTEREST

The authors declare that they have no conflict of interest.

INTRODUCTION

Dementia and stroke rank among the most pressing health issues worldwide (1,2). Cerebral small vessel diseases (SVDs), termed for various pathologies associated with small vessel dysfunction in the brain, have emerged as a central link between these two major co-morbidities. SVDs account for at least 40 % of dementia cases and more than 30 % of strokes (1,3). They encompass multiple distinct diseases that can be separated based on their underlying genetic defects, risk factors, and clinical presentations. Despite the severe nature of these diseases, there are no treatments with proven efficacy against cerebral SVDs.

Major progress has been made in identifying overlapping mechanisms involved in the functional defects of small (parenchymal) arterioles within the brain in response to subarachnoid hemorrhage (SAH) (4) and cerebral autosomal dominant arteriopathy with subcortical infarcts and leukoencephalopathy (CADASIL), a monogenic form of SVD (5). Although, strictly speaking SAH is not a cerebral SVD, an increasing body of evidence suggests that SAH-induced perfusion deficits originate from the parenchymal microvasculature (6–13). These deficits appear to be driven by changes in the balance of matrix metalloproteinase (MMP) activity which supports the novel concept that perturbations of the extracellular matrix can be a point of convergence between these cerebral small vessel pathologies (14). These changes, in turn, alter the number of voltage-gated K^+ (K_V) channels at the arteriolar smooth muscle cells (SMCs) plasma membrane (15–18). The K_V channel superfamily, comprising 12 subfamilies (K_V1–K_V12), is one of the most diverse families of K^+ channels identified to date (19). Molecular cloning of K^+ channels from different cell types has revealed that K_V subfamilies share a common primary structure, reflecting hetero- or homo-multimeric assembly of four pore-forming α subunits and auxiliary β subunits, with the identity of the α subunit being the primary determinant of biophysical and pharmacological properties of individual channels (20–22). In vascular SMCs, K_V channels are active under physiological conditions, and the K^+ efflux that they mediate serves as a key negative feedback control mechanism that opposes moment-to-moment pressure-induced constriction (23). Thus, any increase or decrease in functional K_V channel density on the plasma membrane of arteriolar SMCs is predicted to impact arteriolar diameter.

The potential dire consequences of disrupting the number of functional SMC K_V channels are evident in the two divergent cerebral small vessel pathologies presented here—SAH and CADASIL. In the hemorrhagic stroke (i.e. subarachnoid hemorrhage) model, MMP activation is understood to cause K_V channel endocytosis through activation of the epidermal growth factor receptor (EGFR), resulting in increased vasoconstriction and decreased cerebral blood flow (CBF) (15,16). On the other hand, in a mouse model of CADASIL, an increase in tissue inhibitor of metalloproteinase-3 (TIMP-3) inhibits MMP (ADAM17) activity, leading to an increased number of functional K_V channels in the plasma membrane of arteriolar SMCs and attenuation of vasoconstriction (17,18). These findings support the concept that the number of K_V channels are tuned to provide the appropriate membrane potential control in response to changes in intravascular pressure, and that any change in channel number will adversely affect cerebral arteriolar function.

Here, we weave experimental data and computational modeling to describe small vessel dysfunction after SAH and in CADASIL from a K_V channelopathy perspective, revealing how the "Yin and Yang" of SMC K_V channels—the balance between upregulation and downregulation—is crucial for maintaining parenchymal arteriole (PA) function, CBF and, ultimately, brain health.

1. K_V CHANNELS IN MYOCYTES PROFOUNDLY REGULATE THE MYOGENIC TONE OF BRAIN PARENCHYMAL ARTERIOLES

In vivo, small diameter arteries and arterioles exist in a partially constricted state, largely owing to the vasoconstrictor influence of intravascular pressure. These blood vessels can constrict further as pressure increases and, conversely, dilate when the pressure lessens (24). This response, referred to as myogenic tone, supports CBF autoregulation and protects capillaries from the disruptive effects of high blood pressure (25). Within the brain, myogenic tone also provides the vasodilatory reserve necessary for PAs to locally dilate and increase blood delivery in response to neuronal activity. This use-dependent increase in blood flow, termed functional hyperemia, is supported by a variety of mechanisms collectively referred to as neurovascular coupling (NVC) (1,26–29). Thus, the myogenic response within the cerebral vasculature, specifically in small diameter arterioles, is crucial for CBF control.

This myogenic response can be reproduced *ex vivo* using an arteriography system by increasing intravascular pressure through a cannula inserted into the arteriolar lumen, enabling the study of the molecular players that contribute to this phenomenon. Intravascular pressure causes a graded membrane potential (V_m) depolarization of SMCs that leads to an increase in the open-state probability of voltage-dependent Ca^{2+} channels (VDCCs), thereby enhancing Ca^{2+} influx and ultimately causing myogenic constriction (23,30). In mouse PAs, elevation of luminal pressure from 10 mmHg to 40 mmHg typically causes an 18-mV depolarization of the SMC membrane from −53 mV to −35 mV; the associated doubling in the level of myogenic tone manifests as a constriction that represents approximately a 35–40% decrease in arterial diameter (17).

Like most biological processes, myogenic tone is modulated by negative feedback elements (31). Among them, K^+ channels in SMCs and endothelial cells (ECs) of arterioles can serve as a brake on pressure-induced depolarization and constriction (23). At a physiological extracellular K^+ concentration ($[K^+]_o$) of 3 mM and an intracellular K^+ concentration of 140 mM, the equilibrium potential for K^+ (E_K) is −102.7 mV. At 40 mm Hg, the estimated pressure experienced *in vivo* by cerebral arterioles of this size (32), the SMC membrane potential is about −35 mV, creating a 68-mV driving force for K^+ efflux. Consequently, opening of K^+ channels exerts a rapid and strong hyperpolarizing effect that acts to oppose pressure-induced constriction and, more broadly, provides a vasodilatory influence.

Arteriolar SMCs predominantly express four types of K^+ channels: ATP-sensitive (K_{ATP}), large conductance Ca^{2+}-activated (BK), inward rectifier (K_{IR}), and voltage-gated (K_V) (23,25,33,34). Interestingly, it appears that only K_{IR} and K_V channels are active under physiological conditions in PA SMCs examined *in vitro*. K_{ATP} channels are expressed in large cerebral pial arteries on the surface of the brain (35), but the absence of PA dilation in

response to the K_{ATP} agonist cromakalim suggests a minimal role for this channel type within the brain cortex (36). The apparent lack of functional K_{ATP} channels in PAs is consistent with previous reports that small cerebral arterioles fail to dilate in response to cromakalim (37–40). In many vascular beds, including cortical surface arteries, BK channels are activated by local Ca^{2+}-release events (Ca^{2+} sparks) through ryanodine receptors (RyRs), and exert tonic negative feedback on myogenic tone (41,42). Consistent with this tonic negative feedback element opposing myogenic tone, treatment with BK channel blockers such as paxilline causes significant and sustained constriction of pial cerebral arteries (43). In contrast, BK channel blockade does not alter PA diameter, suggesting that BK channel-mediated K^+ efflux does not constitute a significant feedback mechanism against myogenic tone in PAs under physiological conditions (17,44–46), possibly because Ca^{2+} spark activity is very low in these arterioles (at least in rat and mouse) (47–50). However, considering that BK currents are detectable in isolated PA SMCs (9,46), and can be activated in certain conditions such as acidosis (36,50), a role for BK (and K_{ATP}) channels under all physiological and pathological conditions or in all species is possible.

K_{IR} channels, predominantly $K_{IR}2.1$ channels, are present in both PA SMCs (51–53) and ECs (54). $K_{IR}2.1$ channels conduct strong inward current at V_m negative to E_K and a small outward current that peaks and then decreases as V_m becomes increasingly positive to E_K (23,54). The role of K_{IR} channels in regulating smooth muscle membrane potential has been described in previous reviews (23,34,40). Inhibition of this channel with 30 μM Ba^{2+} or genetic ablation in ECs does not affect PA resting diameter (55). This is likely because channel activity at −35 mV, the resting V_m of PAs at 40 mmHg, is very low, with a conductance, gK_{IR}, about a 10,000-time less than the maximal conductance of this channel (54,56,57). In addition to its aforementioned dependence on V_m, K_{IR} is also activated by external K^+. This enables SMCs and ECs to sense elevations in extracellular K^+ in response to neuronal activity and mediate NVC (7,45,51,55). Therefore, the physiological role of K_{IR} in the brain microcirculation during NVC has been likened to that of a “vascular K^+ electrode”, as defined by Longden and Nelson (54). The voltage and K^+ dependence of K_{IR} synergize in response to small increases in external K^+, leading to dramatic hyperpolarization that is capable of bringing V_m close to E_K and causing near maximal dilation (45,51,55).

We have established that K_V channels play a tonic and profound role in opposing vasoconstrictor influences (e.g., myogenic tone) in PAs from rodent brains (17,58,59). SMC membrane depolarization in response to pressure or vasoconstrictors increases K_V channel open probability, creating a hyperpolarizing K^+ efflux that counterbalances depolarizing current through VDCCs and other Na^+/Ca^{2+} permeable channels to act as a break on vasoconstriction. K_V channels in vascular SMCs show fast activation kinetics in response to membrane potential depolarization, with activation time constants (τ_{act}) on the order of tens of milliseconds (Figure 1A). In addition, the steady-state activation and inactivation properties of K_V allow significant K^+ currents between −40 and +10 mV, implicating K_V channels in the regulation of PA SMC membrane potential at physiological intravascular pressures (Figure 1B). The contribution of K_V channels to the regulation of resting PA diameter is illustrated by the significant constriction caused by inhibition of K_V channels

with 1 mM 4-aminopyridine (4-AP) at physiological pressure (40 mmHg) (Figure 1C) (17,23,58,60,61).

The voltage dependence of K_V channels has been described using a Boltzmann-type steady-state activation term (Figure 2). The characteristics of this voltage dependence—voltage at half-maximal activation ($V_{0.5}$) and slope factor (k_{Kv})—appear to vary significantly among channel subtypes (17,22,23). The involvement of K_V1 channel family members, predominantly $K_V1.2$ and $K_V1.5$ subtypes, in the regulation of arteriolar tone has been documented in the cerebral vasculature of multiple species (17,58,60,62,63). Studies have also reported that K_V2 channels, primarily those of the $K_V2.1$ subfamily, contribute to counteracting myogenic constriction in rat pial cerebral arteries (64–67). Other groups have also provided evidence supporting the contribution of K_V7 channels ($K_V7.1$, $K_V7.4$, and $K_V7.5$ subtypes) to the regulation of pial cerebral arterial diameter (61,68). Regarding intracerebral PAs, a number of lines of experimental evidence support the view that $K_V1.2$ and $K_V1.5$ subtypes are predominantly expressed and primarily regulate PA SMC V_m and arteriolar diameter. First, $V_{0.5}$ values measured in PA SMCs were −3.2 mV in rat (58) and +6 mV in mouse PA SMCs (17), similar to values reported for heteromultimers of $K_V1.2/1.5$ channels (69). In contrast, the $V_{0.5}$ value of K_V7 channels are ~ −30 mV (70). Second, RT-PCR revealed mRNA expression of $K_V1.2$ and $K_V1.5$, but not $K_V1.1$, $K_V1.3$, $K_V1.4$, $K_V1.6$ or $K_V2.1$ in rat PAs (58). Third, stromatoxin, an inhibitor of K_V2 channels (66,71), does not significantly constrict mouse parenchymal arterioles (17). Furthermore, it has been shown that the 4-AP sensitivity of K^+ currents, V_m, and tone are dependent on the expression of $K_V1.2$ and $K_V1.5$ subtypes (60,69,72–74).

2. IMPACT OF PATHOLOGICAL INCREASES (CADASIL) OR DECREASES (SAH) IN PA K_V CHANNEL NUMBERS

The structural organization of the cerebral circulation may explain the formation of regional pathological lesions, which are associated with small vessel dysfunction in SVDs. The two-dimensional network of surface (pial) arteries branches out and dives down into the brain parenchyma as PAs, which ultimately transition into capillary networks of interconnected vessels with a considerable capacity for redirecting blood flow (75). However, PAs upstream of the interconnected capillary networks control the blood supply of a specific volume of brain territory; as such, they represent bottlenecks to blood flow and thus are the element most vulnerable to cerebral SVDs (76,77). PAs also exhibit unique features, including the lack of extrinsic innervation and the presence of astrocytic processes that enwrap almost their entire basolateral surface (78–80). PAs are the last smooth muscle-containing vessels upstream of the capillary bed, and their active luminal diameter in mouse brain is typically < 20 μm—about one-third the width of a human hair. These anatomical features make *ex vivo* experimental approaches for studying their function extremely challenging, which has limited the investigation of this pathophysiologically important vascular bed.

In both SAH and CADASIL, dysregulation of brain PA reactivity precedes the onset of neurological deficits. Using well-established rabbit (15,43,81), rat (6,7) and mouse (12,13) models of SAH, and a transgenic mouse model of CADASIL ($TgNotch3^{R169C}$) in which a human NOTCH3 receptor mutation—the molecular cause of CADASIL—is overexpressed

(17,82), we have discovered that K_V channel activity in PA SMCs is abnormal in both pathological conditions (17,18,59). Although abnormal K_V activity could conceivably reflect changes in channel gating properties or recruitment of new K_V channel family members, our experimental data demonstrated unchanged τ_{act}, $V_{0.5}$, or k in both disease models. Instead, the observed changes in K_V channel activity better correlates with a change in the number of functional channels at the SMC plasma membrane (Figure 2). Specifically, SAH causes a decrease in functional K_V channels and enhanced vasoconstriction. Conversely, CADASIL model mice exhibit an increase in SMC membrane K_V channel numbers and a decrease in cerebral arteriolar tone. One possible mechanism underlying both of these vascular pathologies is altered trafficking of K_V channels. In this context, altered shedding of the epidermal growth factor receptor ligand, HB-EGF, caused by aberrant MMP and/or ADAM (a disintegrin and metalloproteinase) activity, leads to enhanced (SAH) or decreased (CADASIL) EGFR-mediated endocytosis of K_V channels (14–18).

Based on current density data obtained experimentally using the perforated-patch configuration of the patch-clamp technique (17) (Koide & Wellman *unpublished data*), we calculated the number of K_V channels in control (CTL), CADASIL and SAH conditions at a given voltage (−40 mV) using the Goldman–Hodgkin–Katz constant field equation ((83); see (17) for calculation details). We found that the average number of functional K_V channels per myocyte in CTL mice was 3,060 ± 479 (6 cells from 6 animals), a number that increased to 4,970 ± 655 (6 cells from 6 animals) in CADASIL ($TgNotch3^{R169C}$) mice. A comparison of CTL and SAH rats revealed the opposite change, with 3,465 ± 346 channels per myocyte observed in CTL rats (6 cells from 5 animals) compared with 1809 ± 423 in SAH rats (6 cells from 6 animals) (Koide & Wellman *unpublished data*). In each case, the cell capacitances of myocytes were similar, indicating a similar membrane surface area in all three conditions. Therefore, the CADASIL-causing mutation results in a ~57 % increase in K_V channel number, whereas SAH reduces K_V channel number by ~48 %. The differences in K_V current densities between disease and control animals, at different membrane potentials, are depicted in Figure 2. Steady-state K_V current data for CTL and CADASIL mice are fitted to a Boltzmann-type Vm-dependent activation, as previously done (17). The voltage dependency of K_V1 in SAH is predicted based on a 48% reduction in K_V1 conductance relative to CTL. SMC outward K_V1 current increases dramatically at depolarized potentials, reflecting K_V channel opening with depolarization, and current density correlated with the K_V channel number in all conditions.

Given the role of K^+ efflux through K_V channels in opposing pressure-induced membrane depolarization and vasoconstriction, the prediction is that increased (CADASIL) (17) or decreased (SAH) (6,84) K_V channel numbers would alter the degree of negative-feedback control, resulting in hyperpolarization (CADASIL) or depolarization (SAH) of PA SMCs. Consistent with this prediction, experimentally measured V_m was hyperpolarized (−45 mV) (17) and depolarized (−28 mV) (6) in pressurized (40 mmHg) PAs obtained from CADASIL mice and SAH model animals, respectively, compared to CTL groups (−35 mV). The relationship between myogenic tone and membrane potential in CTL, CADASIL and SAH animals is summarized in Figure 3A. At lower intravascular pressure (5 and 10 mmHg), tone and membrane potential did not differ among the three groups. However, as pressure is increased to a more physiological level (40 mmHg), V_m in PAs from CADASIL mice

remained almost 10 mV more hyperpolarized than that in CTL PAs (−45 mV vs. −35 mV), whereas V_m was pulled to −28 mV in SAH (6,17).

We also used a mathematical model of SMC membrane permeability to examine whether the reported changes in V_m could be explained by measured differences in K_V density between CADASIL and SAH animals and CTL groups (6,17) (Figure 3B). This model accounts for the activity of important SMC components, including K_V1, K_{IR}, BK, K_{ATP}, VDCC, and non-selective cation (NSC) channels, as well as Na^+/K^+ ATPases (NaK) and plasma membrane Ca^{2+} pumps (PMCA). Figure 3C demonstrates the effect of increased (CADASIL) and decreased (SAH) K_V channel density under the assumption that the presence of all these other components remains unchanged. Simulations show the effect of increasing transmembrane Na^+ permeability (P_{Na}) accounts for the pressure-induced smooth muscle depolarization in myogenic response, presumably through the opening of stretch activated NSC channels. In agreement with the experimental data (Figure 3A; 5–10 mmHg), the difference in membrane potential between control and disease states is negligible at low P_{Na} current (i.e., low intraluminal pressure) as the contribution of K_V currents to the total transmembrane current diminishes (Figure 3B and 3C). The model predicts that high P_{Na} current (i.e., high intraluminal pressure) leads to depolarization and opening of K_V channels, highlighting the inhibitory role of K_V channels on the myogenic response. A larger number of K_V channels (CADASIL) provide greater negative feedback, resulting in hyperpolarized V_m, less VDCC activity, lower intracellular Ca^{2+}, and less myogenic tone. Conversely, a decrease in the number of K_V channels (SAH) provides less negative-feedback, resulting in more depolarized V_m, increased VDCC activity, higher intracellular Ca^{2+}, and increased myogenic tone. Thus, the model demonstrates that changes in SMC K_V channel density can account for changes in V_m, intracellular Ca^{2+} concentration and myogenic tone, consistent with observations from CADASIL and SAH model animals. In both pathological conditions, a change in the gain of the K_V-mediated negative feedback loop is expected to have profound effects on the responses of arterioles to pressure fluctuations (CBF autoregulation), but also to impact the effect of external K^+ variations during NVC.

3. IMPACT OF SMALL VESSEL PATHOLOGIES ON THE INTERPLAY BETWEEN K_V AND K_{IR} CHANNELS DURING NVC

NVC is the process that links localized neuronal activity in the brain to vasodilation of proximate PAs so as to ensure adequate delivering of oxygen and nutrients to metabolically active regions of the central nervous system. A key component of NVC is the K_{IR}-dependent SMC hyperpolarization and vasodilation that results from modest increases in $[K^+]_o$ within the perivascular space (51,52,85). In isolated PAs, raising $[K^+]_o$ from 3 mM to 8 mM hyperpolarizes the SM V_m to near the new E_K of −76 mV, causing near maximum vasodilation by decreasing Ca^{2+} influx (51). This dramatic V_m hyperpolarization is achieved by K_{IR} activation. Raising $[K^+]_o$ from 3 mM to 8 mM activates K_{IR} channels and results in a 50-fold increase in membrane K^+ permeability (86). In addition to a modest rise in $[K^+]_o$ (e.g., from 3 mM to 8 mM), membrane hyperpolarization itself increases K_{IR} channel activity, causing a rightward shift of the K_{IR} current-voltage relationship and increased outward current amplitude (Figure 4A, left inset) as a result of the positive shift in E_K and an increase in K_{IR} conductance (87). In contrast, a modest rise in $[K^+]_o$ monotonically

decreases outward K_V current due to a reduction in the K^+ chemical gradient (Figure 4A, right inset). Additionally, modest increases in $[K^+]_o$ and the associated K_{IR} channel activation and V_m hyperpolarization would be expected to decrease K_V (and possibly BK) channel open probability. Thus, the interaction between K_{IR} and K_V/BK channels during modest increases in $[K^+]_o$ creates a "tug-of-war" dynamic that would be expected to play an important role in determining SMC K^+ permeability and PA diameter during NVC. Sufficient K_{IR} activation is required to overcome the concurrent decrease in K_V/BK channel activity to produce V_m hyperpolarization and vasodilation. Under physiological conditions, this is the case, with modest increases in $[K^+]_o$ associated with neuronal activation leading to SMC V_m hyperpolarization, vasodilation, and increased local CBF during NVC.

However, evidence indicates impaired NVC in CADASIL (14,18) and SAH (7,13) animal models. Since K_V channel number in PA SMCs is significantly altered in these two pathologies, we used computational modeling to investigate the effect of different K_V channel densities on SMC membrane potential when $[K^+]_o$ is elevated from 3 mM to 8 mM. The current-voltage curves of K_V currents obtained from Figures 1 and 2 are summed with representative PA SMC K_{IR} currents in Figure 4A. Solid lines represent combined K_V and K_{IR} currents at rest ($[K^+]_o$ = 3 mM), and dashed lines represent currents when $[K^+]_o$ is elevated to 8 mM. Shaded areas show the increase in net hyperpolarizing current predicted by shifting $[K^+]_o$ from 3 mM to 8 mM and highlight the V_m window where the K_{IR} influence is dominant (i.e., overcomes the opposing influence of decreased K_V channel activity), producing a net increase in membrane K^+ permeability. Within this V_m range, or "K_{IR} window", hyperpolarization can be achieved during increases in $[K^+]_o$ to 8 mM, whereas outside of this window, the K^+ stimulus will result in unstable membrane potential or even depolarization. Therefore, K^+-induced hyperpolarization is possible when the resting V_m is within the K_{IR} window (Figure 4A shaded areas). Despite differences in K_V current density, our modeling indicates that conditions exist where increasing $[K^+]_o$ from 3 mM to 8 mM would be predicted to hyperpolarize PA SMCs of CTL, CADASIL, and SAH animals (Figure 4B).

In SAH, the prediction is that decreased K_V channel density extends the V_m window where the K_{IR} influence is dominant (Figure 4A red region). This is consistent with our results showing that parenchymal arterioles isolated from the brains of SAH animals and pressurized *ex vivo* dilate in response to modest increases in extracellular K^+ (7). However, SAH is associated with an inversion of NVC in animal models; that is, instead of causing vasodilation, neuronal activation causes vasoconstriction in these animals, both in brain slices and *in vivo* (7,13,88). We have proposed that this inversion of NVC is the result of a pathological increase in basal $[K^+]_o$ reflecting enhanced K^+ efflux by astrocytic endfeet, rather than impaired K_{IR} function. When summed with neurally evoked K^+ efflux, the net elevation in basal $[K^+]_o$ leads to a more depolarized SMC E_K that lies outside of the influence of the K_{IR} window. Thus, the polarity of the vascular response is switched from dilation to constriction due to V_m depolarization and enhanced Ca^{2+} entry through VDCCs (7,13,88).

In CADASIL, the representative model predicts that an increase in K_V channel density reduces the size of the K_{IR} window, but also shifts the window to more hyperpolarized

potentials (Figure 4A, blue region). However, increased K_V channel density in CADASIL model mice also brings resting V_m to more hyperpolarized values (17). According to the simulation, this limits the impact of the increased K_V density on a 8-mM $[K^+]_o$ challenge, and allow K^+-induced dilations to occur. Consistent with this, PAs from CADASIL model mice respond to 8, 15 and 20 mM $[K^+]_o$ with near maximum dilation *ex vivo*, comparable to that in CTL animals (17). Nevertheless, an altered hyperpolarization window may compromise K-induced dilation under some conditions, for example when V_m is more depolarized by the presence of an additional vasoconstrictor. Also, a higher K_V channel density in CADASIL decreases the vasodilatory reserve, because PAs are in a less constricted state compared with controls. This could lead to deficits in vascular autoregulation and the ability of K^+-induced signaling to efficiently redirect blood flow in the vascular network during NVC, as previously reported (14,18).

CONCLUSIONS

Our understanding of cerebral SVDs has advanced greatly over the past decade. Recent work has established the contribution of the yin and yang of the K_V channel balance to the pathological progression of cerebral small vessel dysfunction. Here, we combine data from different animal models with detailed computational modeling to further understand elements of this pathology.

K_V channels, estimated to number 3,000–3,500 per SMC in physiological conditions, play a profound role in regulating PA SMC resting V_m and PA myogenic tone. These channels are sensitive to inhibition by 4-AP, and the current footprint obtained in native PA myocytes aligns with the properties of $K_V1.2$ and $K_V1.5$ subunits, results supported by the expression of mRNAs for these subunits (17,58,59). Changing the number of channels per SMC results in abnormal SMC V_m and myogenic responses—a yin and yang dynamic that helps to account for cerebral microvascular defects in both CADASIL and SAH. Indeed, in addition to being dramatically altered by CADASIL and SAH, K_V channel expression and function in the vascular wall can also be disrupted in the context of other major causes of cerebral SVDs, such as diabetes (58), aging (89), and hypertension (34,90). Thus, targeting K_V1 channels in the vascular wall with the aim of restoring normal hemodynamic function may be a future therapeutic option for such disorders (91).

Secondly, an in-depth characterization of the SMC membrane K^+ permeability control by the K_V−K_{IR} interplay during NVC will enable further advances in our understanding of the impact of SVDs on functional hyperemia. Here, we establish an inroad to this analysis, introducing the new concept that changes in the number of K_V channels impact the tug-of-war between activation of SMC K_{IR} channels and deactivation of K_V channels, which can impair sensitivity to vasoreactive signaling.

Overall, increased K_V channel density in CADASIL narrows the V_m range over which K_{IR} channel can induce dilation, but also brings resting V_m to more hyperpolarized values, partially counteracting the impact of the tug-of-war between K_V and K_{IR} channels at the expense of the vasodilatory reserve. In SAH, decreased K_V channel density leads to depolarization of resting V_m and increases myogenic tone. Compromised NVC in this

disease model may be attributable to high extracellular K^+ levels resulting from excessive K^+ efflux from astrocytes that depolarizes rather than hyperpolarizes SMCs.

FUTURE DIRECTIONS

Recent studies by our group and others have identified a previously unanticipated role for the endothelium, specifically K_{IR} channels in capillary ECs, in sensing neural activity at the capillary level and translating it into a propagating hyperpolarizing electrical signal that dilates upstream arterioles (55,92,93). These findings highlight the importance of conducted hyperpolarization along PAs and hold the promise of resolving controversies regarding SVD-induced neurovascular dysfunction, potentially providing a paradigm-shifting concept. The recent development of cell-type–specific, genetically encoded fluorescent voltage sensors brings the possibility of *in vivo* and *ex vivo* optical electrophysiology within reach (94–97). In the context of electrical signaling between capillaries and arterioles, this may allow us to image how changes in K_V channels alter the regenerative hyperpolarization of the endothelium during NVC. Importantly, CADASIL is caused by mutations in the NOTCH3 receptor, which is expressed not only in vascular SMCs, but also in pericytes (5). The role of pericytes, and their possible dysfunction in NVC, has recently been brought to light by several groups (93,98–101). Although consensus on this point has remained elusive, the increasing number of studies suggests that pericytes provide an additional layer of CBF regulation and therefore could play a key role in facilitating or dampening capillary-to-arteriole signaling. However, whether K_V channels are expressed in pericytes, and whether they are up-regulated in CADASIL and potentially down-regulated in SAH, remains unknown. Resolving these questions may prove critical to a full understanding of the regulation of CBF by K_V channels in the intracerebral microcirculation.

PERSPECTIVE

K_V channels located in SMCs of brain parenchymal arterioles oppose pressure-induced depolarization. Changes in K_V channel density occur in pathological processes that target the brain microcirculation, impairing intracerebral arteriole constriction in response to changes in intravascular pressure. This blunting of a fundamental vascular function is expected to impact cerebral blood flow autoregulation and local dilation in response to neuronal activity (functional hyperemia). Interventions aimed at restoring K_V channel function to improve brain perfusion may thus be a future therapeutic direction in the treatment of cerebral small vessel pathologies.

Acknowledgments

The authors gratefully acknowledge Amanda Mirando and Dr. Adam Strand for their insightful discussion and editorial assistance. This study was supported by a Scientist Development Grant (14SDG20150027 to M.K.) and Grant-in-Aid (17GRNT33700280 to G.C.W.) from the American Heart Association, and grants the Totman Medical Research Trust (to M.T.N.), Fondation Leducq (to M.T.N.), European Union’s Horizon 2020 research and innovation programme (grant agreement No 666881, SVDs@target, to M.T.N.), and National Institutes of Health (P01-HL-095488, R01-HL-121706, R37-DK-053832, 7UM-HL-1207704 and R01-HL-131181 to M.T.N.; and R01-HL-136636 to F.D.).

Abbreviations used

4-AP	4-aminopyridine
$[K^+]_o$	external K^+ concentration
ADAM	a disintegrin and metalloproteinase
BK	large conductance Ca^{2+}- activated K^+ channel
CADASIL	cerebral autosomal dominant arteriopathy with subcortical infarcts and leukoencephalopathy
CBF	cerebral blood flow
CTL	control
EC	endothelial cell
EGFR	epidermal growth factor receptor
E_K	reversal potential for K^+
HB-EGF	heparin-binding epidermal growth factor-like growth factor
K_{ATP}	ATP-sensitive K^+ channel
K_{IR}	inward rectifier K^+ channel
K_V	voltage-gated K^+ channel
MMP	matrix metalloproteinase
NaK	Na^+/K^+ ATPase
NSC	non-selective cation channels
NVC	neurovascular coupling
PA	parenchymal arteriole
PMCA	plasma membrane Ca^{2+} ATPase
RyR	ryanodine receptor
SAH	subarachnoid hemorrhage
SMC	smooth muscle cell
SVD	small vessel disease
TIMP-3	tissue inhibitor of metalloproteinase-3
VDCC	voltage-dependent Ca^{2+} channel
V_m	membrane potential

References

1. Iadecola C. The pathobiology of vascular dementia. Neuron. 2013; 80(4):844–866. [PubMed: 24267647]
2. Yang Z, Lin P-J, Levey A. Monetary costs of dementia in the United States. N Engl J Med. 2013; 369(5):489.
3. Pantoni L. Cerebral small vessel disease: from pathogenesis and clinical characteristics to therapeutic challenges. Lancet Neurol. 2010; 9(7):689–701. [PubMed: 20610345]
4. Bederson JB, Connolly ES, Batjer HH, Dacey RG, Dion JE, Diringer MN, Duldner JE Jr, Harbaugh RE, Patel AB, Rosenwasser RH. Guidelines for the management of aneurysmal subarachnoid hemorrhage: a statement for healthcare professionals from a special writing group of the Stroke Council, American Heart Association. Stroke. 2009; 40(3):994–1025. [PubMed: 19164800]
5. Chabriat H, Joutel A, Dichgans M, Tournier-Lasserve E, Bousser M-G. CADASIL. Lancet Neurol. 2009; 8(7):643–653. [PubMed: 19539236]
6. Nystoriak MA, O'Connor KP, Sonkusare SK, Brayden JE, Nelson MT, Wellman GC. Fundamental increase in pressure-dependent constriction of brain parenchymal arterioles from subarachnoid hemorrhage model rats due to membrane depolarization. Am J Physiol Heart Circ Physiol. 2011; 300(3):H803–H812. [PubMed: 21148767]
7. Koide M, Bonev AD, Nelson MT, Wellman GC. Inversion of neurovascular coupling by subarachnoid blood depends on large-conductance Ca^{2+}-activated K^+ (BK) channels. Proc Natl Acad Sci USA. 2012; 109(21):E1387–1395. [PubMed: 22547803]
8. Østergaard L, Aamand R, Karabegovic S, Tietze A, Blicher JU, Mikkelsen IK, Iversen NK, Secher N, Engedal TS, Anzabi M, Jimenez EG, Cai C, Koch KU, Naess-Schmidt ET, Obel A, Juul N, Rasmussen M, Sørensen JC. The role of the microcirculation in delayed cerebral ischemia and chronic degenerative changes after subarachnoid hemorrhage. J Cereb Blood Flow Metab. 2013; 33(12):1825–1837. [PubMed: 24064495]
9. Wellman GC, Koide M. Impact of subarachnoid hemorrhage on parenchymal arteriolar function. Acta Neurochir Suppl. 2013; 115:173–177. [PubMed: 22890665]
10. Tso MK, Macdonald RL. Subarachnoid hemorrhage: a review of experimental studies on the microcirculation and the neurovascular unit. Transl Stroke Res. 2014; 5(2):174–189. [PubMed: 24510780]
11. Terpolilli NA, Brem C, Bühler D, Plesnila N. Are We Barking Up the Wrong Vessels? Cerebral Microcirculation After Subarachnoid Hemorrhage. Stroke. 2015; 46(10):3014–9. [PubMed: 26152299]
12. Balbi M, Koide M, Schwarzmaier SM, Wellman GC, Plesnila N. Acute changes in neurovascular reactivity after subarachnoid hemorrhage in vivo. J Cereb Blood Flow Metab. 2017; 37(1):178–187. [PubMed: 26676226]
13. Balbi M, Koide M, Wellman GC, Plesnila N. Inversion of neurovascular coupling after subarachnoid hemorrhage in vivo. J Cereb Blood Flow Metab. 2017; 7(11):3625–3634.
14. Joutel A, Haddad I, Ratelade J, Nelson MT. Perturbations of the cerebrovascular matrisome: A convergent mechanism in small vessel disease of the brain? J Cereb Blood Flow Metab. 2016; 36(1):143–157. [PubMed: 25853907]
15. Ishiguro M, Morielli AD, Zvarova K, Tranmer BI, Penar PL, Wellman GC. Oxyhemoglobin-Induced Suppression of Voltage-Dependent K^+ Channels in Cerebral Arteries by Enhanced Tyrosine Kinase Activity. Circ Res. 2006; 99(11):1252–1260. [PubMed: 17068294]
16. Koide M, Penar PL, Tranmer BI, Wellman GC. Heparin-binding EGF-like growth factor mediates oxyhemoglobin-induced suppression of voltage-dependent potassium channels in rabbit cerebral artery myocytes. Am J Physiol Heart Circ Physiol. 2007; 293(3):H1750–H1759. [PubMed: 17557914]
17. Dabertrand F, Krøigaard C, Bonev AD, Cognat E, Dalsgaard T, Domenga-Denier V, Hill-Eubanks DC, Brayden JE, Joutel A, Nelson MT. Potassium channelopathy-like defect underlies early-stage cerebrovascular dysfunction in a genetic model of small vessel disease. Proc Natl Acad Sci USA. 2015; 112(7):E796–E805. [PubMed: 25646445]

18. Capone C, Dabertrand F, Baron-Menguy C, Chalaris A, Ghezali L, Domenga-Denier V, Schmidt S, Huneau C, Rose-John S, Nelson MT, Joutel A. Mechanistic insights into a TIMP3-sensitive pathway constitutively engaged in the regulation of cerebral hemodynamics. Elife. 2016; 5:e17536. [PubMed: 27476853]
19. Gutman GA, Chandy KG, Grissmer S, Lazdunski M, McKinnon D, Pardo LA, Robertson GA, Rudy B, Sanguinetti MC, Stühmer W, Wang X. International Union of Pharmacology. LIII. Nomenclature and molecular relationships of voltage-gated potassium channels. Pharm Rev. 2005; 57(4):473–508. [PubMed: 16382104]
20. Jan LY, Jan YN. Structural elements involved in specific K^+ channel functions. Annu Rev Physiol. 1992; 54(1):537–55. [PubMed: 1562183]
21. Jan LY, Jan YN. Cloned potassium channels from eukaryotes and prokaryotes. Annu Rev Neurosci. 1997; 20(1):91–123. [PubMed: 9056709]
22. Coetzee WA, Amarillo Y, Chiu J, Chow A, Lau D, McCormack T, Moreno H, Nadal MS, Ozaita A, Pountney D, Saganich M, Vega-Saenz de Miera E, Rudy B. Molecular diversity of K^+ channels. Ann N Y Acad Sci. 1999; 868:233–285. [PubMed: 10414301]
23. Nelson MT, Quayle JM. Physiological roles and properties of potassium channels in arterial smooth muscle. Am J Physiol. 1995; 268(4 Pt 1):C799–822. [PubMed: 7733230]
24. Bayliss WM. On the local reactions of the arterial wall to changes of internal pressure. J Physiol. 1902; 28(3):220–231. [PubMed: 16992618]
25. Davis MJ, Hill MA. Signaling mechanisms underlying the vascular myogenic response. Physiol Rev. 1999; 79(2):387–423. [PubMed: 10221985]
26. Faraci FM, Heistad DD. Regulation of large cerebral arteries and cerebral microvascular pressure. Circ Res. 1990; 66(1):8–17. [PubMed: 2403863]
27. Cipolla, MJ. The Cerebral Circulation. San Rafael (CA): Morgan & Claypool Life Sciences; 2009.
28. Fernández-Klett F, Offenhauser N, Dirnagl U, Priller J, Lindauer U. Pericytes in capillaries are contractile in vivo, but arterioles mediate functional hyperemia in the mouse brain. Proc Natl Acad Sci USA. 2010; 107(51):22290–22295. [PubMed: 21135230]
29. Attwell D, Buchan AM, Charpak S, Lauritzen M, MacVicar BA, Newman EA. Glial and neuronal control of brain blood flow. Nature. 2010; 468(7321):232–243. [PubMed: 21068832]
30. Knot HJ, Nelson MT. Regulation of arterial diameter and wall [Ca^{2+}] in cerebral arteries of rat by membrane potential and intravascular pressure. J Physiol. 1998; 508(1):199–209. [PubMed: 9490839]
31. Bernard C. Lectures on the phenomena of life common to animals and plants. 1885
32. Baumbach GL, Sigmund CD, Faraci FM. Cerebral arteriolar structure in mice overexpressing human renin and angiotensinogen. Hypertension. 2003; 41(1):50–55. [PubMed: 12511529]
33. Jackson WF. Potassium Channels in the Peripheral Microcirculation. Microcirculation. 2005; 12(1):113–127. [PubMed: 15804979]
34. Tykocki NR, Boerman EM, Jackson WF. Smooth Muscle Ion Channels and Regulation of Vascular Tone in Resistance Arteries and Arterioles. Compr Physiol. 2017; 7(2):485–581. [PubMed: 28333380]
35. Jansen-Olesen I, Mortensen CH, El-Bariaki N, Ploug KB. Characterization of K_{ATP}-channels in rat basilar and middle cerebral arteries: studies of vasomotor responses and mRNA expression. Eur J Pharmacol. 2005; 523(1–3):109–118. [PubMed: 16226739]
36. Dabertrand F, Nelson MT, Brayden JE. Acidosis dilates brain parenchymal arterioles by conversion of calcium waves to sparks to activate BK channels. Circ Res. 2012; 110(2):285–294. [PubMed: 22095728]
37. McCarron JG, Quayle JM, Halpern W, Nelson MT. Cromakalim and pinacidil dilate small mesenteric arteries but not small cerebral arteries. Am J Physiol. 1991; 261(2 Pt 2):H287–H291. [PubMed: 1908639]
38. McPherson GA, Stork AP. The resistance of some rat cerebral arteries to the vasorelaxant effect of cromakalim and other K^+ channel openers. Br J Pharmacol. 1992; 105(1):51–58. [PubMed: 1534504]

39. Nagao T, Ibayashi S, Sadoshima S, Fujii K, Ohya Y, Fujishima M. Distribution and physiological roles of ATP-sensitive K^+ channels in the vertebrobasilar system of the rabbit. Circ Res. 1996; 78(2):238–243. [PubMed: 8575067]
40. Quayle JM, Nelson MT, Standen NB. ATP-sensitive and inwardly rectifying potassium channels in smooth muscle. Physiol Rev. 1997; 77(4):1165–1232. [PubMed: 9354814]
41. Brayden JE, Nelson MT. Regulation of arterial tone by activation of calcium-dependent potassium channels. Science. 1992; 256(5056):532–535. [PubMed: 1373909]
42. Nelson MT, Cheng H, Rubart M, Santana LF, bonev AD, Knot HJ, Lederer WJ. Relaxation of arterial smooth muscle by calcium sparks. Science. 1995; 270(5236):633–637. [PubMed: 7570021]
43. Koide M, Nystoriak MA, Krishnamoorthy G, OConnor KP, Bonev AD, Nelson MT, Wellman GC. Reduced Ca^{2+} spark activity after subarachnoid hemorrhage disables BK channel control of cerebral artery tone. J Cereb Blood Flow Metab. 2011; 31(1):3–16. [PubMed: 20736958]
44. Horiuchi T, Dietrich HH, Hongo K, Dacey RG. Mechanism of Extracellular K^+-Induced Local and Conducted Responses in Cerebral Penetrating Arterioles. Stroke. 2002; 33(11):2692–2699. [PubMed: 12411663]
45. Girouard H, Bonev AD, Hannah RM, Meredith A, Aldrich RW, Nelson MT. Astrocytic endfoot Ca^{2+} and BK channels determine both arteriolar dilation and constriction. Proc Natl Acad Sci USA. 2010; 107(8):3811–3816. [PubMed: 20133576]
46. Hannah RM, Dunn KM, Bonev AD, Nelson MT. Endothelial SK_{Ca} and IK_{Ca} channels regulate brain parenchymal arteriolar diameter and cortical cerebral blood flow. J Cereb Blood Flow Metab. 2011; 31(5):1175–1186. [PubMed: 21179072]
47. Westcott EB, Jackson WF. Heterogeneous function of ryanodine receptors, but not IP_3 receptors, in hamster cremaster muscle feed arteries and arterioles. Am J Physiol Heart Circ Physiol. 2011; 300(5):H1616–H1630. [PubMed: 21357503]
48. Westcott EB, Goodwin EL, Segal SS, Jackson WF. Function and expression of ryanodine receptors and inositol 1,4,5-trisphosphate receptors in smooth muscle cells of murine feed arteries and arterioles. J Physiol. 2012; 590(8):1849–1869. [PubMed: 22331418]
49. Dabertrand F, Mironneau J, Macrez N, Morel J-L. Full length ryanodine receptor subtype 3 encodes spontaneous calcium oscillations in native duodenal smooth muscle cells. Cell Calcium. 2008; 44(2):180–189. [PubMed: 18207571]
50. Dabertrand F, Nelson MT, Brayden JE. Ryanodine receptors, calcium signaling, and regulation of vascular tone in the cerebral parenchymal microcirculation. Microcirculation. 2013; 20(4):307–316. [PubMed: 23216877]
51. Filosa JA, Bonev AD, Straub SV, Meredith AL, Wilkerson MK, Aldrich RW, Nelson MT. Local potassium signaling couples neuronal activity to vasodilation in the brain. Nat Neurosci. 2006; 9(11):1397–1403. [PubMed: 17013381]
52. Longden TA, Dabertrand F, Hill-Eubanks DC, Hammack SE, Nelson MT. Stress-induced glucocorticoid signaling remodels neurovascular coupling through impairment of cerebrovascular inwardly rectifying K^+ channel function. Proc Natl Acad Sci USA. 2014; 111(20):7462–7467. [PubMed: 24808139]
53. Povlsen GK, Longden TA, Bonev AD, Hill-Eubanks DC, Nelson MT. Uncoupling of neurovascular communication after transient global cerebral ischemia is caused by impaired parenchymal smooth muscle Kir channel function. J Cereb Blood Flow Metab. 2016; 36(7):1195–1201. [PubMed: 27052838]
54. Longden TA, Nelson MT. Vascular inward rectifier K^+ channels as external K^+ sensors in the control of cerebral blood flow. Microcirculation. 2015; 22(3):183–196. [PubMed: 25641345]
55. Longden TA, Dabertrand F, Koide M, Gonzales AL, Tykocki NR, Brayden JE, Hill-Eubanks D, Nelson MT. Capillary K^+-sensing initiates retrograde hyperpolarization to increase local cerebral blood flow. Nat Neurosci. 2017; 20(5):717–726. [PubMed: 28319610]
56. Quayle JM, McCarron JG, Brayden JE, Nelson MT. Inward rectifier K^+ currents in smooth muscle cells from rat resistance-sized cerebral arteries. Am J Physiol. 1993; 265(5 Pt 1):C1363–1370. [PubMed: 7694496]

57. Knot HJ, Zimmermann PA, Nelson MT. Extracellular K^+-induced hyperpolarizations and dilatations of rat coronary and cerebral arteries involve inward rectifier K^+ channels. J Physiol. 1996; 492(Pt 2):419–430. [PubMed: 9019539]
58. Straub SV, Girouard H, Doetsch PE, Hannah RM, Wilkerson MK, Nelson MT. Regulation of intracerebral arteriolar tone by K_V channels: effects of glucose and PKC. Am J Physiol Heart Circ Physiol. 2009; 297(3):C788–796.
59. Koide M, Wellman GC. SAH-induced suppression of voltage-gated K^+ (K_V) channel currents in parenchymal arteriolar myocytes involves activation of the HB-EGF/EGFR pathway. Acta Neurochir Suppl. 2013; 115:179–184. [PubMed: 22890666]
60. Albarwani S, Nemetz LT, Madden JA, Tobin AA, England SK, Pratt PF, Rush NJ. Voltage-gated K^+ channels in rat small cerebral arteries: molecular identity of the functional channels. J Physiol. 2009; 551(3):751–763.
61. Zhong XZ, Harhun MI, Olesen SP, Ohya S, Moffatt JD, Cole WC, Greenwood IA. Participation of KCNQ (K_V7) potassium channels in myogenic control of cerebral arterial diameter. J Physiol. 2010; 588(17):3277–3293. [PubMed: 20624791]
62. Cheong A, Dedman AM, Beech DJ. Expression and function of native potassium channel [$K_V$alpha1] subunits in terminal arterioles of rabbit. J Physiol. 2001; 534(Pt 3):691–700. [PubMed: 11483700]
63. Cheong A, Dedman AM, Xu SZ, Beech DJ. $K_V$alpha1 channels in murine arterioles: differential cellular expression and regulation of diameter. Am J Physiol Heart Circ Physiol. 2001; 281(3):H1057–H1065. [PubMed: 11514271]
64. Amberg GC, Rossow CF, Navedo MF, Santana LF. NFATc3 regulates $K_V2.1$ expression in arterial smooth muscle. J Biol Chem. 2004; 279(45):47326–47334. [PubMed: 15322114]
65. Amberg GC, Santana LF. K_V2 channels oppose myogenic constriction of rat cerebral arteries. Am J Physiol Heart Cell Physiol. 2006; 291(2):C348–C356.
66. Zhong XZ, Abd-Elrahman KS, Liao CH, El-Yazbi AF, Walsh EJ, Walsh MP, Cole WC. Stromatoxin-sensitive, heteromultimeric $K_V2.1/K_V9.3$ channels contribute to myogenic control of cerebral arterial diameter. J Physiol. 2010; 588(22):4519–4537. [PubMed: 20876197]
67. Nieves-Cintron M, Nystoriak MA, Prada MP, Johnson K, Fayer W, Dell'Acqua ML, Scott JD, Navedo MF. Selective down-regulation of $K_V2.1$ function contributes to enhanced arterial tone during diabetes. J Biol Chem. 2015; 290(12):7918–7929. [PubMed: 25670860]
68. Jepps TA, Olesen SP, Greenwood IA. One man's side effect is another man's therapeutic opportunity: targeting K_V7 channels in smooth muscle disorders. Br J Pharmacol. 2012; 168(1): 19–27.
69. Kerr PM, Clement-Chomienne O, Thorneloe KS, Chen TT, Ishii K, Sontag DP, Walsh MP, Cole WC. Heteromultimeric $K_V1.2–K_V1.5$ channels underlie 4-aminopyridine-sensitive delayed rectifier K^+ current of rabbit vascular myocytes. Circ Res. 2001; 89(11):1038–44. [PubMed: 11717161]
70. Blom SM, Schmitt N, Jensen HS. The Acrylamide (S)-2 As a positive and negative modulator of K_V7 channels expressed in xenopus laevis oocytes. PLoS One. 2009; 4(12):e8251. [PubMed: 20011514]
71. Escoubas P, Diochot S, Célérier M-L, Nakajima T, Lazdunski M. Novel tarantula toxins for subtypes of voltage-dependent potassium channels in the K_V2 and K_V4 subfamilies. Mol Pharmacol. 2002; 62(1):48–57. [PubMed: 12065754]
72. Thorneloe KS, Chen TT, Kerr PM, Grier EF, Horowitz B, Cole WC, Walsh MP. Molecular composition of 4-aminopyridine-sensitive voltage-gated K^+ channels of vascular smooth muscle. Circ Res. 2001; 89(11):1030–1037. [PubMed: 11717160]
73. Plane F, Johnson R, Kerr P, Wiehler W, Thorneloe K, Ishii K, Chen T, Cole W. Heteromultimeric K_V1 channels contribute to myogenic control of arterial diameter. Circ Res. 2005; 96(2):216–224. [PubMed: 15618540]
74. Chen TT, Luykenaar KD, Walsh EJ, Walsh MP, Cole WC. Key role of K_V1 channels in vasoregulation. Circ Res. 2006; 99(1):53–60. [PubMed: 16741158]
75. Shih AY, Rühlmann C, Blinder P, Devor A, Drew PJ, Friedman B, Knutsen PM, Lyden PD, Mateo C, Mellander L, Nishimura N, Schaffer CB, Tsai PS, Kleinfeld D. Robust and fragile aspects of

cortical blood flow in relation to the underlying angioarchitecture. Microcirculation. 2015; 22(3): 204–218. [PubMed: 25705966]

76. Nishimura N, Schaffer CB, Friedman B, Lyden PD, Kleinfeld D. Penetrating arterioles are a bottleneck in the perfusion of neocortex. Proc Natl Acad Sci USA. 2007; 104(1):365–370. [PubMed: 17190804]
77. Shih AY, Blinder P, Tsai PS, Friedman B, Stanley G, Lyden PD, Kleinfeld D. The smallest stroke: occlusion of one penetrating vessel leads to infarction and a cognitive deficit. Nat Neurosci. 2013; 16(1):55–63. [PubMed: 23242312]
78. Simard M, Arcuino G, Takano T, Liu QS, Nedergaard M. Signaling at the gliovascular interface. J Neurosci. 2003; 23(27):9254–62. [PubMed: 14534260]
79. Hamel E. Perivascular nerves and the regulation of cerebrovascular tone. J Appl Physiol. 2005; 100(3):1059–1064.
80. Iadecola C, Nedergaard M. Glial regulation of the cerebral microvasculature. Nat Neurosci. 2007; 10(11):1369–1376. [PubMed: 17965657]
81. Link TE, Murakami K, Beem-Miller M, Tranmer BI, Wellman GC. Oxyhemoglobin-induced expression of R-type Ca^{2+} channels in cerebral arteries. Stroke. 2008; 39(7):2122–8. [PubMed: 18436877]
82. Joutel A, Monet-Leprêtre M, Gosele C, Baron-Menguy C, Hammes A, Schmidt S, Lemaire-Carrette B, Domenga V, Schedl A, Lacombe P, Hubner N. Cerebrovascular dysfunction and microcirculation rarefaction precede white matter lesions in a mouse genetic model of cerebral ischemic small vessel disease. J Clin Invest. 2010; 120(2):433–445. [PubMed: 20071773]
83. Alvarez O, Latorre R. The enduring legacy of the “constant-field equation” in membrane ion transport. J Gen Physiol. 2017; 149(10):911–920. [PubMed: 28931632]
84. Koide M, Wellman GC. SAH-induced MMP activation and K_V current suppression is mediated via both ROS-dependent and ROS-independent mechanisms. Acta Neurochir Suppl. 2015; 120:89–94. [PubMed: 25366605]
85. Zhang C, Tabatabaei M, Bélanger S, Girouard H, Moeini M, Lu X, Lesage F. Astrocytic endfoot Ca^{2+} correlates with parenchymal vessel responses during 4-AP induced epilepsy: An in vivo two-photon lifetime microscopy study. J Cereb Blood Flow Metab. 2017 271678X17725417.
86. Longden TA, Hill-Eubanks DC, Nelson MT. Ion channel networks in the control of cerebral blood flow. J Cereb Blood Flow Metab. 2016; 36(3):492–512. [PubMed: 26661232]
87. Shah AK, Cohen IS, Datyner NB. Background K^+ current in isolated canine cardiac Purkinje myocytes. Biophys J. 1987; 52(4):519–525. [PubMed: 2445390]
88. Pappas AC, Koide M, Wellman GC. Purinergic signaling triggers endfoot high-amplitude Ca^{2+} signals and causes inversion of neurovascular coupling after subarachnoid hemorrhage. J Cereb Blood Flow Metab. 2016; 36(11):1901–1912. [PubMed: 27207166]
89. Kang LS, Kim S, Dominguez JM, Sindler AL, Dick GM, Muller-Delp JM. Aging and muscle fiber type alter K^+ channel contributions to the myogenic response in skeletal muscle arterioles. J Applied Physiol. 2009; 107(2):389–398. [PubMed: 19407249]
90. Cox RH. Changes in the expression and function of arterial potassium channels during hypertension. Vasc Pharmacol. 2002; 38(1):13–23.
91. Wulff H, Castle NA, Pardo LA. Voltage-gated potassium channels as therapeutic targets. Nat Rev Drug Discov. 2009 Dec; 8(12):982–1001. [PubMed: 19949402]
92. Chen BR, Kozberg MG, Bouchard MB, Shaik MA, Hillman EMC. A critical role for the vascular endothelium in functional neurovascular coupling in the brain. J Am Heart Assoc. 2014; 3(3):e000787–7. [PubMed: 24926076]
93. Wei HS, Kang H, Rasheed I-YD, Zhou S, Lou N, Gershteyn A, McConnell ED, Wang Y, Richardson KE, Palmer AF, Xu C, Wan J, Nedergaard M. Erythrocytes are oxygen-sensing regulators of the cerebral microcirculation. Neuron. 2016; 91(4):851–862. [PubMed: 27499087]
94. Gong Y, Huang C, Li JZ, Grewe BF, Zhang Y, Eismann S, Schnitzer MJ. High-speed recording of neural spikes in awake mice and flies with a fluorescent voltage sensor. Science. 2015; 350(6266): 1361–6. [PubMed: 26586188]

95. Marshall JD, Li JZ, Zhang Y, Gong Y, St-Pierre F, Lin MZ, Schnitzer MJ. Cell-type-specific optical recording of membrane voltage dynamics in freely moving mice. Cell. 2016; 167(6):1650–1662. e15. [PubMed: 27912066]

96. St-Pierre F, Marshall JD, Yang Y, Gong Y, Schnitzer MJ, Lin MZ. High-fidelity optical reporting of neuronal electrical activity with an ultrafast fluorescent voltage sensor. Nat Neurosci. 2014; 17(6): 884–889. [PubMed: 24755780]

97. Lou S, Adam Y, Weinstein EN, Williams E, Williams K, Parot V, et al. Genetically targeted all-optical electrophysiology with a transgenic cre-dependent optopatch mouse. J Neurosci. 2016; 36(43):11059–11073. [PubMed: 27798186]

98. Hall CN, Reynell C, Gesslein B, Hamilton NB, Mishra A, Sutherland BA, O'Farrell FM, Buchan AM, Lauritzen M, Attwell D. Capillary pericytes regulate cerebral blood flow in health and disease. Nature. 2014; 508(7494):55–60. [PubMed: 24670647]

99. Hill RA, Tong L, Yuan P, Murikinati S, Gupta S, Grutzendler J. Regional blood flow in the normal and ischemic brain is controlled by arteriolar smooth muscle cell contractility and not by capillary pericytes. Neuron. 2015; 87(1):95–110. [PubMed: 26119027]

100. Kisler K, Nelson AR, Rege SV, Ramanathan A, Wang Y, Ahuja A, Lazic D, Tsai PS, Zhao Z, Zhou Y, Boas DA, Sakadžić S, Zlokovic BV. Pericyte degeneration leads to neurovascular uncoupling and limits oxygen supply to brain. Nat Neurosci. 2017; 20(3):406–416. [PubMed: 28135240]

101. Underly RG, Levy M, Hartmann DA, Grant RI, Watson AN, Shih AY. Pericytes as inducers of rapid, matrix metalloproteinase-9-dependent capillary damage during ischemia. J Neurosci. 2017; 37(1):129–140. [PubMed: 28053036]

102. Kapela A, Bezerianos A, Tsoukias NM. A mathematical model of Ca^{2+} dynamics in rat mesenteric smooth muscle cell: agonist and NO stimulation. J Theor Biol. 2008; 253(2):238–260. [PubMed: 18423672]

103. Cipolla MJ, Sweet J, Chan S-L, Tavares MJ, Gokina N, Brayden JE. Increased pressure-induced tone in rat parenchymal arterioles vs. middle cerebral arteries: role of ion channels and calcium sensitivity. J Applied Physiol. 2014; 117(1):53–59. [PubMed: 24790017]

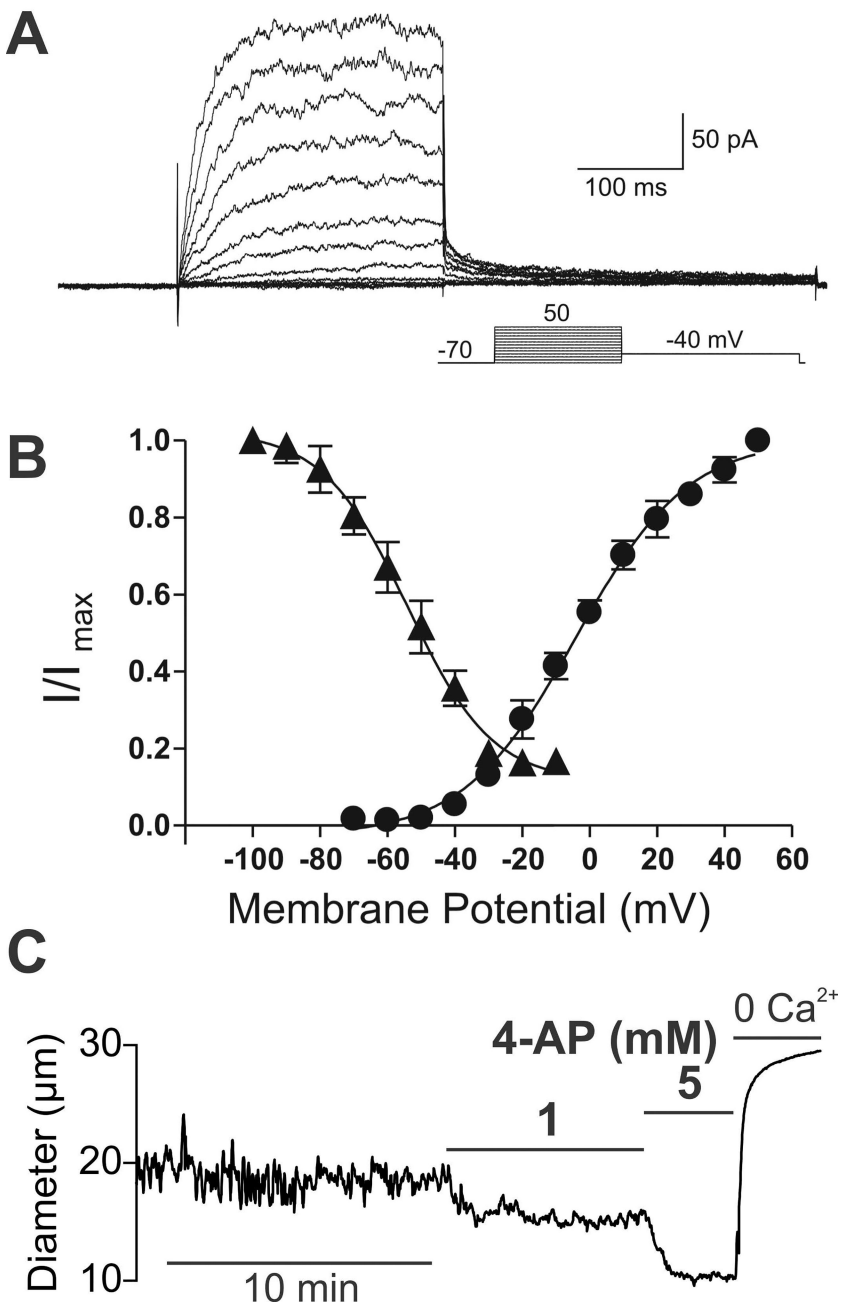

Figure 1. K_V channels exert a tonic dilatory influence on the diameter of intracerebral arterioles

(**A**) Families of K_V currents from an isolated arteriolar smooth muscle cell elicited by voltage pulses from −70 mV to +50 mV in the presence of 100 nM iberiotoxin to inhibit large conductance (BK) currents. (**B**) steady-state activation (circles) and inactivation (triangles) properties of K_V currents measured from isolated arteriolar smooth muscle cells. Solid lines, Boltzmann fits to the data. (**C**) Typical recording of the internal diameter of a pressurized parenchymal arteriole (40 mm Hg) showing the constriction caused by the perfusion of the K_V blocker 4-AP, 1 and 5 mM. **A** and **B** are from (58) and **C** is from (17).

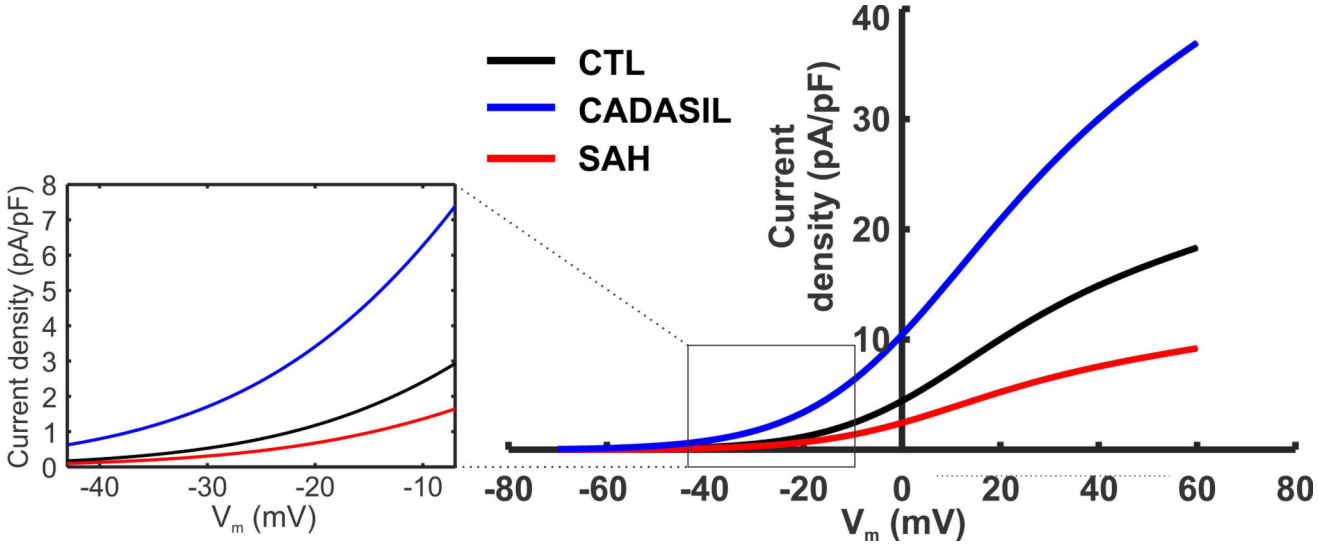

Figure 2. Steady state K_V current density in PA SMCs from normal and diseased animal models

Steady state K_V current densities for CTL, CADASIL (TgNotch3^{R169C}), and SAH models are fitted using a linear equation $I_{Kv}=\frac{1}{c_m}mG_{Kv}(V_m-E_K)$ with a Boltzmann-type activation term $m=\frac{1}{1+\exp(-(\frac{V_m-V_{Kv,0.5}}{k_{kv}}))}$, from experimental data (17) and Koide & Wellman *unpublished data*. C_m is the membrane capacitance; V_m is the membrane potential; G_{Kv} is the whole-cell conductance of K_V channels; E_K is the reversal potential for K^+. At physiological membrane potentials pA differences in K_V currents are predicted (Figure inset). Model parameters: G_{kv} = 1.6 [nS]; $V_{Kv,0.5}$ = 6 [mV]; k_{kv} = 14 [mV] for control; G_{kv} = 0.8 [nS]; $V_{Kv,0.5}$ = 6 [mV]; k_{kv} = 14 [mV] for SAH; and G_{kv} = 3.2 [nS]; $V_{Kv,0.5}$ = 2.6 [mV]; k_{kv} = 15.8 [mV] for CADASIL model; C_m = 12.8 [pF]; $[K^+]_i$ = 150 [mM]; $[K^+]_o$ = 3 [mM].

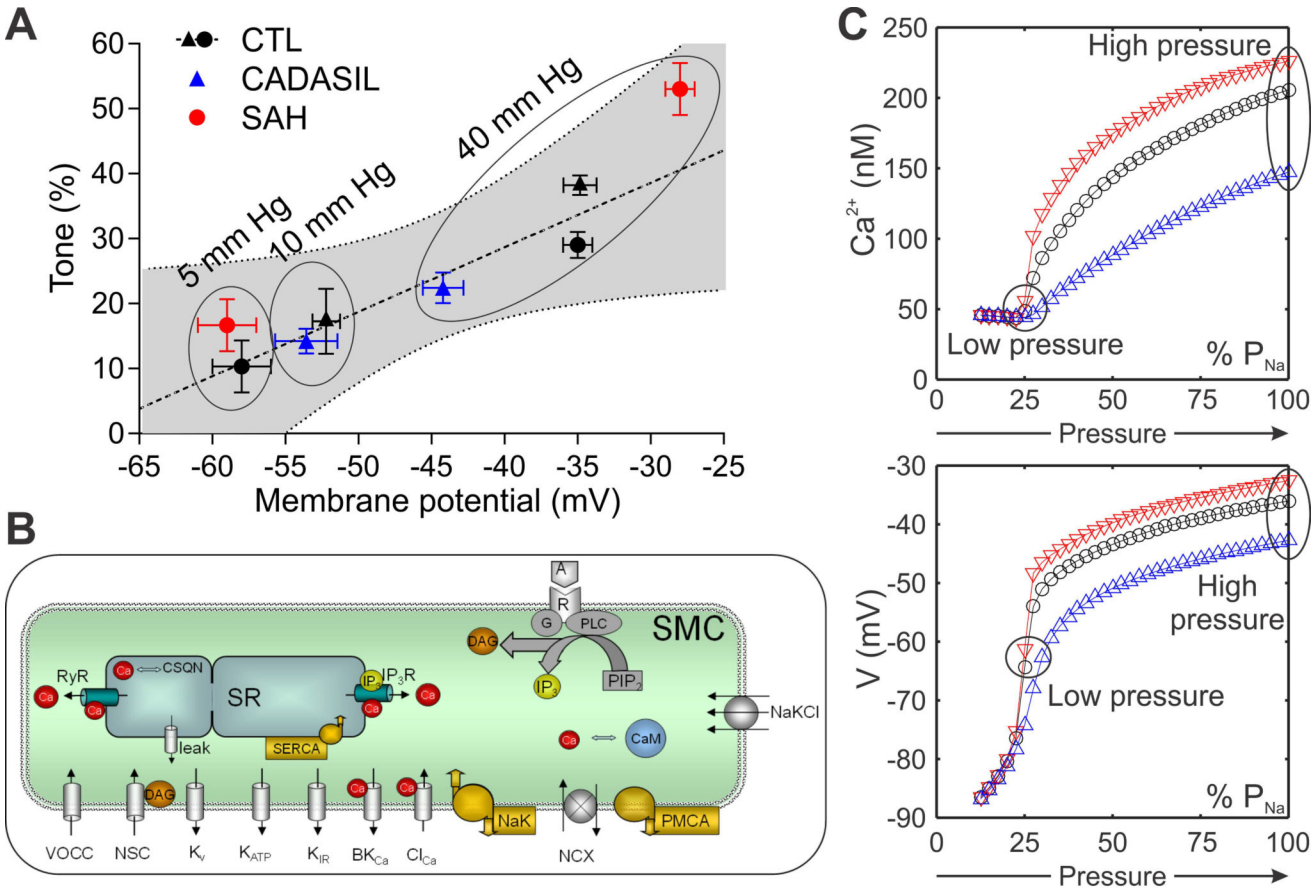

Figure 3. Relationship between myogenic tone and membrane potential

(**A**) Values of membrane potential and myogenic tone at different intravascular pressure (mm Hg) from CADASIL (TgNotch3^{R169C}, blue triangles) and SAH (red circles) animals are consistent with the linear regression obtained from CTL animals (black triangles represent CTL mice from (17) and black circles represent CTL rats from (6)) showing a similar relationship between tone and membrane potential. (**B**) A detailed model of SMC membrane potential and Ca^{2+} dynamics was adapted from (102) and modified by incorporating the K_V1 current of PA SMCs from CTL animals (Figure 2), while adjusting other transmembrane currents (K_{IR}, NSC, VDCC, NaK, PMCA) to produce resting V_m and Ca^{2+} concentration in agreement with experimental data (17,103). The effect of altered K_V1 channel density in CADASIL (blue triangles) and SAH (red triangles) was examined assuming all other model parameters remain the same as in CTL (black circles). (**C**) The effect of increasing pressure was simulated by depolarizing SMC membrane through increasing Na^+ permeability (P_{Na}). Model simulations, in agreement with the corresponding experiments in (A), show differences between CADASIL and SAH animals in V_m (bottom) and Ca^{2+} (top) as pressure increases and highlight the inhibitory role of K_V channels and the effect K_V channel density on myogenic tone. Parameters as in reference (102) except: $P_{VDCC}=6.3\times10^{-5}$ cm/s; $P_{NaNSC}=1.23\times10^{-6}$ cm/s; I_{PMCA}=8.58 pA; I_{NaK}=7.76 pA/pF; G_{KIR} = 0.5 nS/(mM)$^{0.5}$; $G_{Na,leak}$=0.12 nS; C_m = 12.8 pF.

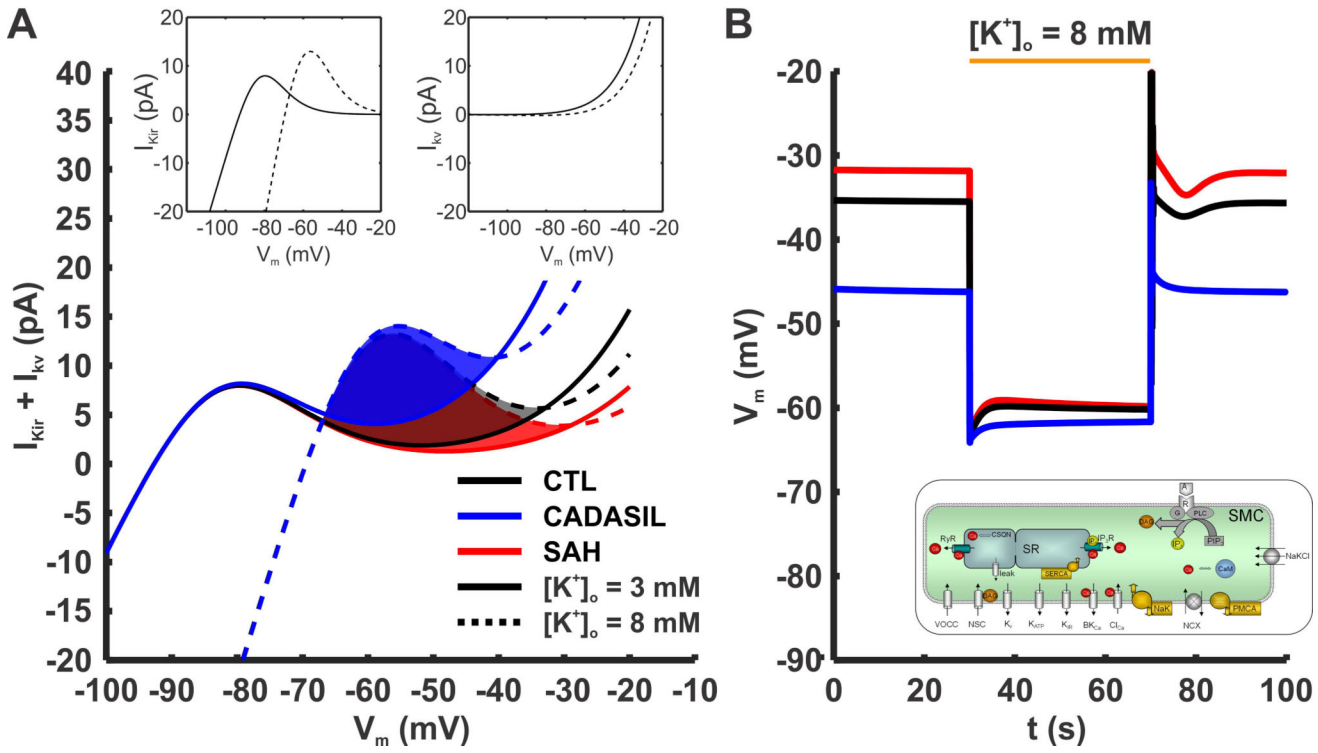

Figure 4. Effect of PA SMC K_V current density and the interplay with K_{IR} current on V_m dynamics at rest and during potassium challenge

(**A**) Combined contribution of K_{IR} and K_v currents in healthy and diseased models during rest and $[K^+]_o$ stimulus. Activation of K_{IR} current by $[K^+]_o$ and hyperpolarization is accounted: $$I_{\mathrm{Kir}}=\frac{G_{\mathrm{Kir,max}}(V_m-E_K)}{1+\exp(\frac{(V_m-V_{K_{\mathrm{IR}},0.5})}{k_{\mathrm{Kir}}})};G_{\mathrm{Kir,max}}=G_{\mathrm{Kir}}[K^+]_o^{0.5}$$ where $G_{kir,max}$ is the maximal K_{IR} conductance. Solid lines show the sum of the two currents at rest, and dashed lines are during elevation of $[K^+]_o$ from 3 to 8 mM. The shaded regions show the range of voltages within which K_{IR} current increases more than K_V current decreases during the K^+ stimulus, i.e. the resting V_m window where the K^+ challenge will result in hyperpolarization. As K_V current density increases (from SAH, red lines; to CTL black lines; to CADASIL, blue lines) the window shrinks in size and shifts to more hyperpolarized potentials. (**B**) Representative simulation using the model of PA SMCs from Figure 3. SMCs from CTL (black line), CADASIL (blue line) and SAH (red line) conditions hyperpolarize following an increase in extracellular K^+, $[K^+]_o$, from 3 mM to 8 mM. The change in membrane potential is less for CADASIL as a result of the more hyperpolarized resting V_m prior to the K^+ challenge. G_{KIR} = 0.76 [nS/(mM)$^{0.5}$]; k_{KIR} = 7 [mV]; $V_{KIR,0.5}$= E_K+12 [mV].